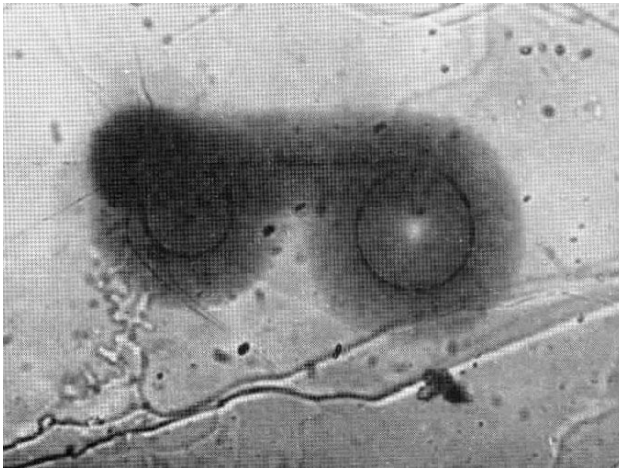


## 'Spectacle' array of $^{210}\text{Po}$ halo radiocentres in biotite: a nuclear geophysical enigma

**POLONIUM** radiohaloes occur widely and not infrequently (total about  $10^{15}$ - $10^{20}$ ) in Precambrian rocks but their existence has so far defied satisfactory explanation based on accepted nucleocosmogeochemical theories<sup>1</sup>. Do Po haloes imply that unknown processes were operative during the formative period of the Earth? Is it possible that Po haloes in Precambrian rocks represent extinct natural radioactivity<sup>2</sup> and are therefore of cosmological significance? A detailed comparison between an unusual array of Po halo radiocentres and U—Th halo radiocentres is presented here as bearing on the above questions.

Generally, radiohaloes occur in one of several mineralogical contexts<sup>1,2,3</sup>. First, as single haloes around discrete inclusions well isolated from other mineral defects and haloes; second, as single haloes around discrete inclusions lodged in conduits or cleavage cracks; third, as single haloes randomly spaced in clusters (sometimes overlapping); fourth, as vein haloes which formed from a continuous distribution of radioactivity (apparently deposited from hydrothermal solutions) along a conduit; and fifth, as line haloes, which surround, not conduits or cracks, but genuine single inclusions which are long (for example, 25  $\mu\text{m}$ ) compared with their width (perhaps 1  $\mu\text{m}$ ). Large, amorphous, coloured regions without discrete inclusions are not haloes.



**Fig. 1** "Spectacle" array of  $^{210}\text{Po}$  haloes in biotite. Halo radius, 18.5  $\mu\text{m}$ .

A striking exception<sup>1</sup> to this classification is the 'spectacle' coloration pattern (Fig. 1), which exhibits two almost circular rings of inclusions joined by a linear array of inclusions. As far as we know this is unlike any group of haloes previously seen. This geometrical arrangement of halo radiocentres, found in a Precambrian biotite from Silver Crater Mine, Faraday Township, Ontario, exhibits true radiohalo characteristics.

First, the coloration is identical to that of normal haloes found about 300  $\mu\text{m}$  away in the same mica specimen. Second, the three-dimensional nature of the halo pattern was demonstrated when the specimen (initially about 50  $\mu\text{m}$  thick) was cleaved; both halves revealed matching 'spectacle' coloration patterns, the only difference being the presence of the inclusion array in one half and its absence in the other half. Third, the radius of the coloration band (18.5  $\mu\text{m}$ ) implied an origin from  $^{210}\text{Po}$   $\alpha$  decay. Mass spectrometric and X-ray fluorescence methods were used to ascertain whether this was indeed a Po halo array.

Before applying these techniques to the 'spectacle' halo, we established that ion-microprobe mass analyses and scanning electron microscope X-ray fluorescence (SEM-XRF) studies of 'normal' or 'standard' halo radiocentres (those formed from both Tl and Th  $\alpha$  decay) yielded data consistent with the visual means of identification. Several U—Th haloes (see, for example, photo insert, Fig. 2) found in a Precambrian pegmatitic mica from Rossi, New York, were analyzed by X-ray and ion-probe techniques. Several U—Th halo radiocentres were chosen which contained only U, Th and Pb in any significant abundance, thereby virtually eliminating any molecular ion interference in the Pb—Th—U region ( $m/e = 204$ —238) in the ion probe.

That the mica matrix<sup>5</sup> yielded insignificant molecular ion currents in the region  $m/e$  160—320 is evident from the data in the lower portion of Fig. 2. In contrast, the recorded spectra of a U—Th inclusion (upper left portion of Fig. 2) revealed a significant number of ion counts accumulated in 12 passes of the regions  $m/e$  204—209 and (with a different scale)  $m/e$  232—240. Total ion counts are tabulated just above the two spectra. The scans on the Pb—Bi region ( $m/e$  204—209) lasted for several minutes and were taken before the scans (equal time) on the U—Th region.

Exact  $^{206}\text{Pb}/^{238}\text{U}$  and  $^{208}\text{Pb}/^{232}\text{Th}$  ratios are not obtainable from the ion count data in Fig. 2 because variable U and Th concentrations were observed as the ion probe beam sputtered away the inclusion; accurate ratios could be obtained by simultaneously accumulating counts in the region 204—238 provided that the greater secondary ion yield of U and Th as compared with Pb is taken into account. On the other hand, the separate Pb and U isotope ratios are meaningful. Note, for example, that after subtraction of background counts at  $m/e$  240 from the total counts at  $m/e$  235 and 238, the 235/238 value (0.76) satisfactorily approximates (considering the relatively small number of counts collected) the natural U isotopic ratio,  $^{235}\text{U}/^{238}\text{U} = 0.72$ . The absence of a peak at 204 shows there is little or no common lead in the inclusion and therefore, that the 206/207 ratio is that of  $^{206}\text{Pb}/^{207}\text{Pb}$  as derived from *in situ* U decay.

Also shown in Fig. 2 are the SEM-XRF spectra of the mica matrix and the U—Th halo radiocentre, both of which correlate well (with the exception of the low  $Z$  and low abundance elements in the former) with the respective ion-probe spectra. Only U, Th and Pb are exclusively in the inclusion.

The ion-microprobe mass spectrum of the mica matrix surrounding the 'spectacle' halo was nearly identical to the mica spectrum shown in Fig. 2 and is not repeated in Fig. 3. Figure 3 (top centre) shows the portion  $m/e = 160$ —264 of the ion-microprobe spectrum (vertical log scale) of several of the inclusions. Also shown is the actual ion-probe trace of the important region from  $m/e = 204$ —210 using a linear vertical scale and an expanded horizontal scale. There is no significant ion current above  $m/e = 209$ ; that is, no significant ion signals were detected at any of the prominent U and Th peaks: 238( $\text{U}^+$ ), 254( $\text{UO}^+$ ), 232( $\text{Th}^+$ ) and 248( $\text{ThO}^+$ ). No  $m/e = 204$  was detected above background (1 c.p.s.), and the 206/207 mass ratio was  $\approx 20$  (206 signal  $\approx 2,000$  c.p.s.).

Figure 3 also shows SEM-XRF spectra of the surrounding mica and of one of the Po halo radiocentres. Lead is the only

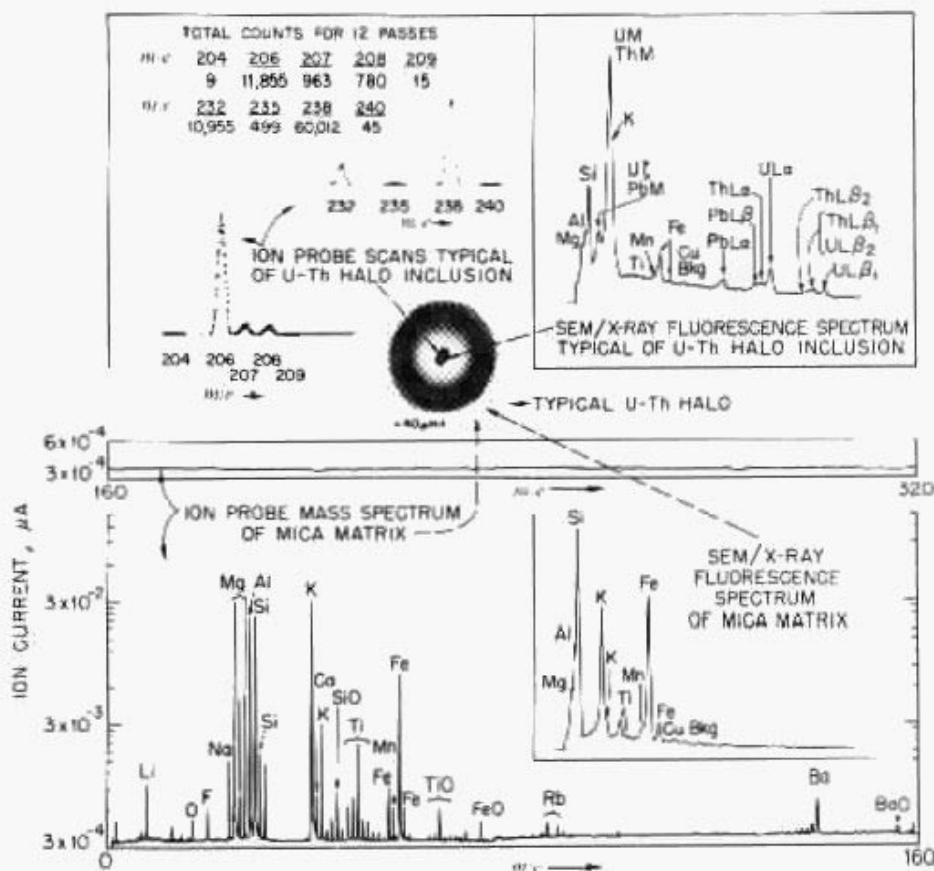


Fig. 2 Ion microprobe and XRF comparison between mica matrix and U-Th halo inclusion.

204–238, the 206, 207 and 208 peaks are interpreted as Pb isotopes and 209 as  $^{209}\text{Bi}$ .  $^{204}\text{Pb}$ , a constituent of both common and primordial Pb, is missing (no 204 peak), implying that the 'spectacle' halo inclusions analysed contained no detectable Pb

of either of these types. Absence of the 232, 235 and 238 peaks is interpreted as showing the inclusions contain virtually no  $^{232}\text{Th}$ ,  $^{235}\text{U}$  or  $^{238}\text{U}$  and, therefore, no radiogenic  $^{208}\text{Pb}$ ,  $^{207}\text{Pb}$  or  $^{206}\text{Pb}$  derived from the *in situ* decay of these isotopes. The 207 and 208

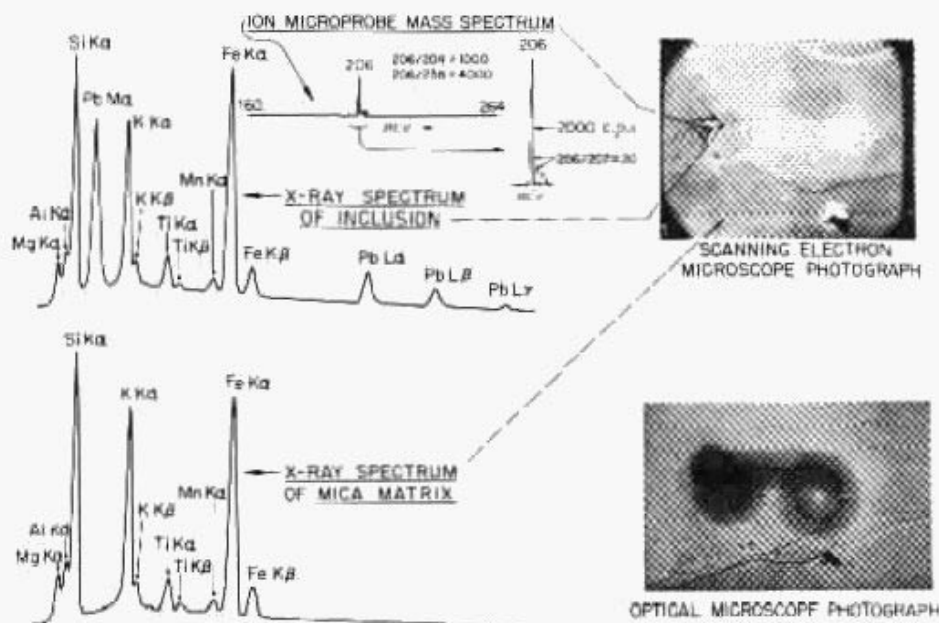


Fig. 3 Ion microprobe and SEM-XRF spectra of mica matrix and  $^{210}\text{Po}$  halo inclusions.

element detectable in this radiocentre exclusive of the mica; some adjacent radiocentres revealed Bi as well. The use of two different instruments, and longer counting times, account for the slightly different X-ray spectra in Figs 2 and 3. The excellent resolution of the SEM showed the Pb-rich areas to coincide exactly with the Po halo radiocentres which are visible both in ordinary transmitted (Fig 1) and reflected light microscopy. Regions as close as 1  $\mu\text{m}$  to the radiocentres showed virtually no Pb or Bi, implying little if any diffusion loss from the inclusions.

As the X-ray data definitely show Pb (and sometimes Bi) in the 'spectacle' halo radiocentres, and as there is no evidence for any molecular ion contribution in the region from  $m/e =$  peaks are therefore attributed to  $^{207}\text{Pb}$  and  $^{208}\text{Pb}$ , perhaps arising from the decay of minute amounts of  $^{211}\text{Bi}$  and  $^{212}\text{Bi}$  within the inclusions<sup>5,6</sup>. The  $^{209}\text{Bi}$  is considered to be primordial.

The outstanding feature of the mass analysis is the prominent 206 signal which, when attributed to the presence of  $^{206}\text{Pb}$  in the inclusions, fits perfectly with the prediction based on ring structure measurements, that is, that the  $^{206}\text{Pb}$  is radiogenically derived, not from U or Th, but directly from  $^{210}\text{Po}$   $\alpha$  decay. In this respect, the large difference in the 206/238 ( $^{206}\text{Pb}/^{236}\text{U}$ ) ratio between the 'spectacle' halo and the U—Th halo (Figs 2 and 3) is especially significant. Clearly the 'spectacle' halo resulted from  $^{210}\text{Po}$   $\alpha$  decay; an explanation for its geometry is still under study.

Because the Pb isotope in these inclusions is not explicable as any combination of common, primordial, or from *in situ* Pb derived radiogenically *in situ* from U or Th, we conclude that a different type of Pb, derived from Po  $\alpha$  decay, exists in nature. Supportive evidence comes from electron-probe and ion-probe analyses of a  $^{218}\text{Po}$  halo radiocentre found in a mica from the Iveland District, Norway, which yielded a  $^{206}\text{Pb}/^{207}\text{Pb}$  ratio of 23. This is consistent with that expected from  $^{218}\text{Po}$   $\alpha$  decay to  $^{206}\text{Pb}$ . Such a Pb ratio is impossibly high based on normal isotopic  $^{238}\text{U}/^{235}\text{U}$  decay, the theoretical maximum being 21.8.

Other investigations have shown varying mixtures of U-derived and Po-derived Pb may occur in the same radiocentre, for there exists an almost continuous halo spectrum stretching from 'pure' U to 'pure' Po haloes. Only a few (<0.01) Po haloes in biotite may survive the delicate sectioning process necessary for SEM X-ray analysis.

Just as important as the existence of a new type of lead is the question of whether Po haloes which occur in a granitic or pegmatitic environment (for example, in mica, fluorite or cordierite, can be explained by accepted models of Earth history<sup>1</sup>. (R. V. G. has found other  $^{210}\text{Po}$  haloes that differ essentially from those in granites—unpublished information.)

This research has been sponsored by the United States Atomic Energy Commission under contract with Union Carbide Corp. and by Columbia Union College with an assistance grant from the National Science Foundation. Thanks are due to R. I. Gait and J.A. Mandarino, Royal Ontario Museum, Louis Moyd, National Museum of Canada, and G. Switzer, United States National Museum, for providing specimens.

#### ROBERT V. GENTRY

Chemistry Division,  
Oak Ridge National Laboratory,

#### L. D. HULETT

Analytical Chemistry Division,  
Oak Ridge National Laboratory

#### S. S. CRISTY

#### J. F. MCLAUGHLIN

Laboratory Development Department,  
Oak Ridge Y-12 Plant,  
Oak Ridge, Tennessee 37830

#### J. A. MCHUGH

Knolls Atomic Power Laboratory,  
Schenectady, New York 12301

#### MICHAEL BAYARD

McCrone Associates,  
2820 Michigan Street,  
Chicago, Illinois 60616

#### Received July 31, 1974.

<sup>1</sup> Gentry, R. V., *Science*, **184**, 62 (1974).

<sup>2</sup> Kohnan, T. P., *Ann. N. Y. Acad. Sci.*, **62**, 503 (1956).

<sup>3</sup> Henderson, G. H., Mushkat, C. M., and Crawford, D. P., *Proc. R. Soc.*, **A158**, 199 (1934); Henderson, G. H., and Turnbull, L. G., *ibid.*, **145**, 582 (1934); Henderson, G. H., and Bateson, S., *ibid.*, 573 (1934).

<sup>4</sup> Gentry, R. V., *Ann. Rev. Nucl. Sci.*, **23**, 347 (1973).

<sup>5</sup> Gentry, R. V., Cristy, S. S., McLaughlin, J. F., and McHugh, J. A., *Nature*, **244**, 282 (1973).

<sup>6</sup> Gentry, R. V., *Science*, **173**, 727 (1971).